The Cryosphere Discuss., 7, 3001–3042, 2013
www.the-cryosphere-discuss.net/7/3001/2013/
doi:10.5194/tcd-7-3001-2013

The Cryosphere Discussions
Open Access

A satellite-based snow cover climatology (1985–2011) for the European Alps derived from AVHRR data

F. Hüsler[1], T. Jonas[2], M. Riffler[1], J. P. Musial[1], and S. Wunderle[1]

[1]Oeschger Center and Institute of Geography, University of Bern, Bern, Switzerland
[2]WSL Institute for Snow and Avalanche Research SLF, Davos Dorf, Switzerland

Received: 31 May 2013 – Accepted: 6 June 2013 – Published: 24 June 2013

Correspondence to: F. Hüsler (fabia.huesler@giub.unibe.ch)

Published by Copernicus Publications on behalf of the European Geosciences Union.

Abstract

Seasonal snow cover is of great environmental and socio-economic importance for the European Alps. Therefore a high priority has been assigned to quantifying its temporal and spatial variability. Complementary to land-based monitoring networks, optical satellite observations can be used to derive spatially comprehensive information on snow cover extent. For understanding long-term changes in alpine snow cover extent, the data acquired by the Advanced Very High Resolution Radiometer (AVHRR) sensors mounted onboard the National Oceanic and Atmospheric Association (NOAA) and Meteorological Operational satellite (MetOp) platforms offer a unique source of information.

In this paper, we present the first space-borne 1 km snow extent climatology for the Alpine region derived from AVHRR data over the period 1985–2011. The objective of this study is twofold: first, to generate a new set of cloud-free satellite snow products using a specific cloud gap-filling technique and second, to examine the spatiotemporal distribution of snow cover in the European Alps over the last 27 yr from the satellite perspective. For this purpose, snow parameters such as snow onset day, snow cover duration (SCD), melt-out date and the snow cover area percentage (SCA) were employed to analyze spatio-temporal variability of snow cover over the course of 3 decades. On the regional scale, significant trends were found toward a shorter SCD at lower elevations in the south-east and south-west. However, our results do not show any significant trends in the monthly mean SCA over the last 27 yr. This is in agreement with other research findings and may indicate a deceleration of the decreasing snow trend in the Alpine region.

Given the importance of mountain regions for climate change assessment, this study recommends the complementary use of remote sensing data for long-term snow applications. It bears the potential to provide spatially and temporally comprehensive snow information for use in related research fields or to serve as a reference for climate models.

1 Introduction

Today, the importance of alpine snow cover is beyond controversy: it not only represents a significant geophysical variable in the climate system (IPCC, 2007) but also plays a major role in regulating mountain ecosystems (Jones, 2001; Jonas et al., 2008) and influences hydrological regimes (EEA, 2009). Furthermore, the alpine snow pack is considered an important economic factor, which has a large impacts on tourism (Elsasser and Bürki, 2002; Agrawala, 2007) and hydropower production (Hänggi and Weingartner, 2012). Likewise, snow is a critical variable in flood forecasting (Jasper et al., 2002) and reservoir management but also for avalanche warning and public safety services (Fuchs and Brandl, 2005). Therefore, it is of paramount interest to determine and quantify its variability on various spatial and temporal scales. In this context, "snow cover" has been officially declared an Essential Climate Variable (ECV) by the Global Climate Observing System (GCOS) and high priority is assigned to enhancing and maintaining snow cover observations (WMO, 2010, 2011).

Snow parameters and their spatio-temporal distribution are commonly monitored using three methodologies (or combinations of them), each one having its strengths and limitations. Ground-based monitoring networks provide valuable long time series data to investigate temporal variability and long-term trends (Beniston, 1997; Scherrer et al., 2004; Scherrer and Appenzeller, 2006; Laternser and Schneebeli, 2003; Marty, 2008; Hantel and Hirtl-Wielke, 2007; Marty and Meister, 2012). However spatial analyses are constrained to dense station networks. Modeling approaches provide another possibility to increase our knowledge of the cryospheric processes. For snow cover, models range from considering simple relations between precipitation and air temperature (Rango and Martinec, 1995) through to complex physical interactions at different spatial scales (Marks et al., 1999; Lehning et al., 2006). However, while conceptual models require regional calibration, complex process-oriented models are often challenged by the enormous requirements as to input data (Magnusson et al., 2011). In addition, they may still rely on a set of assumptions and auxiliary data, which by

TCD
7, 3001–3042, 2013

themselves include uncertainties. Complementary rather than substitutionally, satellite remote sensing (RS) has become an attractive option to study snow cover variability on a wide range of spatial and temporal scales (König et al., 2001; Dietz et al., 2012; Metsämäki et al., 2012). The major advantage of visible RS is its ability to provide area-wide and spatially comprehensive surface information with a regular repeatability of measurements, even in remote areas. However, limitations include cloud cover impeding surface view, the obstruction of snow by dense vegetation as well as the surface heterogeneity in mountain areas, which complicates the interpretation of RS data. Nevertheless, climatological snow cover studies based on RS data have been successfully compiled on regional to hemispherical scales (Robinson and Frei, 2000; Armstrong and Brodzik, 2001; Zhao and Fernandes, 2009; Foppa and Seiz, 2012).

Starting in 1960, RS technology has undergone rapid changes. With advanced sensor technologies, new dimensions of monitoring snow properties have been achieved and the measurement accuracy has increased (Rees, 2005; Nolin, 2011; Dietz et al., 2012). Indeed, the exceptional value of older sensors lies in their unique long-term dataset. Among these, the AVHRR instrument provides the longest record of visible satellite imagery on a daily basis. The University of Bern has archived daily full resolution AVHRR data over Europe for almost 30 yr (1984–2012). Using AVHRR for long-term climate studies, however, means having to properly deal with the many limitations of this sensor, such as calibration uncertainties and changing channel configuration, which have been addressed in various studies (James and Kalluri, 1994; Cihlar et al., 2004; Heidinger et al., 2010; Gutman and Masek, 2012). The main difficulty therefore lies in the appropriate raw data processing, which is a key requirement to access the full potential of the archived data.

This study presents and analyzes the first consistent space-borne 1 km snow coverage climatology derived from AVHRR instruments over the European Alps for the period 1985–2011. A robust and validated snow retrieval algorithm (Hüsler et al., 2012) was applied to derive real surface variability with consistent results. Hence, the objectives of this study are (1) to compile a set of cloud-free satellite snow composites using a spatial and temporal gap-filling method and (2) to employ these composites to analyze the spatiotemporal snow cover variability in the Alpine region over the last three decades. This is done using snow parameters such as snow onset day, snow cover duration, snow melt-out date, and the snow cover area percentage.

Given the need for spatial representations of the alpine snow cover and its variations for many research fields, including hydrological and ecological applications, socio-economic questions or albedo parametrization in climate models, this dataset is considered a powerful contribution to a regional climate observing system.

2 Data

2.1 Study area

The topography and delineation of the Alpine region as defined by the Alpine Convention (http://www.alpconv.org/index_en, accessed December 2012) are shown in Fig. 1. The complex topography of the European Alps, coupled with the varying altitudinal and climatic conditions, essentially influences the spatial and temporal occurrence and duration of the snow cover. Consequently, it allows us to investigate highly variable climatic conditions on comparatively short horizontal and vertical distances. For our investigations, the study area was additionally subdivided into four distinct climatic regions which are assumed to reflect different snow cover regimes. These subregions are defined according to the statistical regionalization of different climate elements such as precipitation and temperature (Auer et al., 2007). The most distinct climate border is found along the Central Alpine crest. It represents the continental transition zone from the temperate westerly to the Mediterranean subtropical climate. A second continental scale climate border is identified between the (western) oceanic influenced and the (eastern) continental part of Eurasia. This rather uniform border roughly follows the 12th degree eastern longitude and was not found to be caused by any topographic feature (Auer et al., 2007). The size, altitudinal distribution and climatic classification of the study area and each subregion are listed in Table 1.

2.2 AVHRR dataset

The dataset consists of daily 1 km gridded binary snow cover maps generated from a full-resolution AVHRR data archive, which is unique in its form as it represents the longest and most comprehensive full-resolution RS dataset for the European Alps (Hüsler et al., 2011). The snow detection relies on a threshold approach that capitalizes on the spectral properties of snow in the visible and the near infrared spectrum and it is applicable to any kind of AVHRR sensor generation with consistent results. Originally developed for rather flat areas in Canada (Khlopenkov and Trishchenko, 2007), the algorithm was adapted and optimized for use in complex terrain. The modifications of the original algorithm basically include changes in the thresholds, taking into account land cover types and topographic features such as terrain shadow. In addition, a distinct snow probability map comes with each snow map, providing a pixel-wise probability index of snow occurrence based on logistic regression. A detailed description of the algorithm itself and an extensive validation of the product can be found in Hüsler et al. (2012). The overall classification accuracy of snow detection was found to be good, with an average probability of detection of up to 90 % depending on land cover class, acquisition geometry, and aspect.

The number of available scenes per season is displayed in Fig. 2. To constrain the influence of the snow's distinct bidirectional distribution function effects (Wiscombe and Warren, 1980) and strong shadowing due to low sun angles we only use midday and early-afternoon overpasses. This, however, comes at the cost of two small data gaps in 1994 as well as in 2000, when only early-morning platforms were in orbit. Additionally, the maximum sensor zenith angle was constrained to 35° since the snow mask accuracy was found to decrease with the distance to nadir.

An irregular distribution over such a long period is inevitable, mainly due to a varying number of platforms simultaneously in orbit. This needs to be taken into account in time series applications. Generally, there is an increasing trend in the data availability. While the number of scenes from 1985 to 1989 can primarily be used for temporal applications relying on monthly mean data, the record provides an almost complete daily coverage from 1989–2002 and reaches a maximum of 2–3 overpasses per day from 2003–2011. Therefore, depending on the type of application, two different time periods are considered in the study at hand. First, 1985–2011 for the monthly mean snow cover time series and second, 1991–2011 for spatial applications relying on daily data coverage.

2.3 Gridded station dataset

As a reference dataset, a gridded snow depth climatology based on in situ measurements (cf. Rhyner et al., 2002; Jonas et al., 2009) available for Switzerland was employed. This data set consists of daily snow depth measurements from 133 stations for the period of 1989–2009 and is therefore considered stable over time (see also Hüsler et al., 2012). To avoid the problem of comparing point scale data (stations) to area scale data (satellite), the snow depth data were mapped to the AVHRR grid using a snow data assimilation scheme based on Auer et al. (2004). Different thresholds are suggested in literature to infer snow coverage from measured snow depth, which is assumed to approximately represent a 50 % fractional snow cover in complex alpine terrain at 1 km resolution. These commonly range from 1 cm (Parajka and Bloeschl, 2006; Foppa and Seiz, 2012) over 4 cm (Wang et al., 2009) to 5 cm (Romanov et al., 2002). Here, a threshold of 5 cm was used to calculate snow cover percentage to avoid shallow snow depth or patchy snow cover not detectable by satellite. Slopes steeper than 20° were excluded from the analyses as they are not considered being well represented in the two data sets.

3 Methods

3.1 Snow mask gap-filling procedure

One major drawback of optical sensors such as AVHRR is their inability to provide surface information under cloudy conditions. This strongly limits the number of useful snow observations as abundant cloud cover is present in the Alpine region, particularly during the winter season.

Various techniques have been developed to reduce cloud-covered pixels from optical imagery. They mostly include spatial and temporal filtering techniques (i.e., Voigt, 2000; Gafurov and Bárdossy, 2009; Parajka et al., 2010), multi-day maximum snow cover composites, or a combination of acquisitions from similar sensors (i.e., Parajka and Blöschl, 2008; Wang et al., 2008; Hall et al., 2010).

In this study, we use a combination of spatial and temporal gap-filling techniques to mitigate the influence of clouds. In the first step we applied straightforward spatial filtering using the regional snowline estimation (SNOWL) method as suggested by Parajka et al. (2010). This procedure reclassifies cloudy pixels to snow or snow-free land, according to their position, relative to the current snowline elevation. In their publication, the accuracy of this method was assessed using 754 climate stations and it was found that the SNOWL method provides robust snow cover mapping over Austria, even under abundant cloud cover of 90 % (Parajka et al., 2010). To avoid blurring regional differences by assuming one snowline elevation for the whole Alpine region, the reclassification was done separately for each of the four distinct climatic regions (cf. Sect. 2.1).

In the second step, a forward (pixel value of closest clear-sky observation in the forward time direction) and a backward (pixel value of closest clear-sky observation in the backward time direction) gap-filling procedure (Foppa and Seiz, 2012) was carried out over a period of 10 days in both directions. After testing different temporal lags, the number of 10 days was found to provide the best results when considering the trade-off between remaining clouds and the “blurring” of snow information. Especially during winter, frequent cloud cover and fog persistence could not be eliminated satisfactorily using shorter periods. For the final product, the mean between the two values was taken. This is based on the assumption that the under or over estimation in one time direction is minimized by averaging the results from the forward and the backward gap-filling procedures (Foppa and Seiz, 2012).

3.2 Snow cover parameters

In order to analyze the spatiotemporal variation of snow cover, the following parameters were employed:

to estimate the temporal distribution, the snow cover area percentage (SCA) is a frequently used measure (Armstrong and Brodzik, 2001; Gao et al., 2012). It is defined as the percentage area of a certain reference area (i.e., the Alpine region) covered by snow at a specific point in time. For time series analysis, standardized anomalies with respect to month are computed using:

$$A = (X - \mu)/\sigma, \tag{1}$$

where X is the single monthly value, μ is the long-term mean and σ the standard deviation of the respective month.

The snow cover duration (SCD) is another parameter of broad interest, i.e., for winter tourism, water resource management, agricultural and disaster/flood forecasting. To make our results comparable in a broader context, we adapted the measures suggested by Wang and Xie (2009) and Gao et al. (2012). Using the gap-filled data product, we calculated the annual SCD using all available scenes within a hydrological year starting from 1 October to 30 September as follows:

$$\mathrm{SCD} = \sum_{i=0}^{N} D_i, \tag{2}$$

where N is the total number of scenes within the hydrological year; D_i is the actual pixel value for a one day composite within the period (0 for snow-free, 1 for snow).

TCD
7, 3001–3042, 2013

This parameter basically counts pixel-wise the number of snow values and represents the total number of snow days for one hydrological year. The SCD anomalies provide a measure for the difference between the SCD value of a specific year compared to the long-term mean SCD. Likewise, monthly anomalies represent the difference between the actual monthly value and the long-term mean value for the respective month.

In the context of an anticipated climate change, the snow cover onset, as well as melt out timing, represent valuable indicators. Following the explanations of Wang and Xie (2009), these measures are captured in the Snow Cover Onset Day (SCOD), which represents the first day of snow occurrence for a certain pixel,

$$\mathrm{SCOD} = D - \mathrm{SCD}', \tag{3}$$

where SCD′ is the snow cover duration within the period from 1 October (DOY = 274 or 275) to 31 December (DOY = 365 or 366) and D is the Day Of Year (DOY) of 31 December (DOY = 365 or 366), when the area is supposed to be covered by snow. The Snow Cover Melting Day (SCMD), that is, the last day with snow occurrence within a pixel, is defined as:

$$\mathrm{SCMD} = D + \mathrm{SCD}'', \tag{4}$$

where SCD′′ is the snow cover duration within the period from 1 January (DOY = 1) to 31 May (DOY = 151 or 152) and D is 1 January (DOY = 1) of the respective year.

Since these measures rely on the continuous availability of data, errors might arise from single missing scenes. Therefore, only the period of 1991–2011 (excluding the years 1995 and 2001) was considered when the amount of adjacent missing values is reasonably small (< 10). The SCOD and SCMD parameters are most meaningful in areas with stable snow cover, i.e., with a continuous snow cover between the onset and the melt-out. For regions with intermittent snow cover, SCOD and SCMD count the snow days within the indicated period but are not affected by repeated short-term snow events that often occur at lower elevations. A slightly modified approach was tested, setting the SCOD (SCMD) date when a pixel was snow-covered for a certain

TCD
7, 3001–3042, 2013

number of consecutive days. This, however, resulted in single missing or gap-filled scenes which completely distorted the parameters. Therefore, the measures described here were concluded to be useful bearing in mind that the results are of most interest in those regions with continuous seasonal snow cover.

4 Results

4.1 Gap-filled product

The results of the spatial and temporal filtering process for all available scenes for the period January to April 2006 are illustrated in Fig. 3. This analysis was restricted to Switzerland due to the limited extent of the station reference dataset (see Sect. 2.3). The values of the relative area percentage of the classes: snow, snow-free, cloud and invalid pixels per scene change considerably from the unfiltered scenes (a) to the final filtered scenes (c). As an intermediate step, panel (b) shows the relative redistribution of the classes after the spatial gap-filling but before the temporal gap-filling. Merely minor changes become apparent as this step affects only a small number of the pixels, which are primarily located at high altitudes. Panel (d) shows the difference between the forward and the backward gap-filling direction and the averaged value as compared to the gridded station dataset. Only minor differences in the range of 0–10 % between the averaged value and the reference dataset are found. Therefore the gap-filling procedure is considered appropriate.

Even though spatial and temporal interpolation techniques are powerful tools to retrieve more comprehensive surface information, they also introduce uncertainties into the dataset. Designed to make assumptions about conditions beneath the cloud cover, confidence in a surface value decreases proportionally to the length of the cloud cover persistence. As introduced by Hall et al. (2010), a piece of associated cloud-persistence-information for each pixel is provided as an indicator of confidence in the actual pixel value. The cloud persistence values are low during clear conditions indicating high confidence and they increase with persisting cloudy conditions, resulting in lower confidence. Furthermore, for interpretation, one should consider that products based on gap filling methods only provide estimates of cloud free observations of multiple days (±10 days) and pixel values remain subject to this uncertainty. Likewise, initial uncertainties arise from erroneous classification of clouds as snow and vice versa since the two features exhibit very similar spectral properties and remain difficult to discriminate.

Based on this satellite-based snow cover climatology, the spatiotemporal distribution of snow in the Alps over the last two decades is analyzed with respect to spatial distribution, annual and inter-annual variations in snow cover. The time period considered for each application is indicated.

4.2 Spatial distribution of snow cover (1991–2011)

The long-term annual means (1991–2011) for the parameters SCD, SCOD and SCMD for the Alpine region are displayed in Fig. 4 for each AVHRR pixel. The overall uncertainty lies at ±10 days as reported in Sect. 3.1. Generally, altitude is the main influencing factor due to the temperature gradient decreasing with height. All parameters clearly follow the distinct topography. Focussing on SCD (Fig. 4, left panel), the highest areas are shown in dark red indicating year-round (365 days) snow cover above approximately 2900 m a.s.l. The SCD gradually decreases along the altitudinal steps and reaches a minimum of < 25 days in the lowest regions in the south-west as well as in the south towards the Po Valley in Northern Italy. Similarly, regional differences become apparent. For example, the SCD in the south-western parts is much lower (i.e., 40 days on average) than in the north-eastern part (i.e., 75 days on average), even though lying at about the same altitude range (i.e., between 600 and 700 m a.s.l.). This occurs presumably due to different climatic influences (see Sect. 2.1). Yet, these regional differences decrease toward higher altitudes and the SCD becomes similar in magnitude in all regions.

TCD
7, 3001–3042, 2013

Since the SCD is closely linked – at least in altitudes with stable snow cover – to the SCOD, when snow starts to accumulate, and to the SCMD, when snow disappears, a similar pattern can be found in the center and right panels of Fig. 4. Even though the topography clearly emerges in both maps, regional differences such as the west-east, but also south-north gradient, are present as well. A comparatively more blurred pattern is observed in the SCOD map as this measure depends not only on temperature but also on availability of precipitable water in atmosphere. The SCMD, in contrast, shows very subtle differences indicating a slow and gradual decrease of snow between January (with values between 25 and 59 at low altitudes) and the end of May (at altitudes of around 2300 m a.s.l., values of 225–244) caused by the spring temperature increase. These results are perfectly in line with observations made by Jonas et al. (2008) illustrating that SCOD (SCMD) shows little (high) correlation with elevation over time.

4.3 Annual variation of snow cover (1985–2011)

The amount of snow present in the Alps varies considerably over the course of one year. The seasonal snow cover generally starts to increase in November, reaches a maximum between January and February and starts to melt out in mid-March. By the end of May, almost all snow has disappeared except for the very high areas lying above 2500 m a.s.l.

Figure 5 quantitatively illustrates the monthly statistics averaged over the period 1985–2011 retrieved from the satellite record. Focussing on the entire Alpine region, the snow cover peaks in January and February with a monthly median of 68 %, that corresponds to an area of approximately 155 000 km^2. During the melting season, it gradually decreases, reaching a minimum extent during August and September, when only the perennial snow and ice remain on the ground (approximately 2600 km^2 ± 25 % in the Alps according to Fontana et al. (2010)). The Inter Quartile Range (IQR), defined as the distance between the 75th percentile and the 25th percentile, is largest in February, March and November, when the highest inter-annual variability is observed

TCD
7, 3001–3042, 2013

due to variations of SCA in the transition zone (approximately 700–2100 m a.s.l.). As expected, the smallest variation is found during summer when a minimum snow cover is present, which is reasonably stable over the whole record's period.

Even though the subregions are not comparable in terms of absolute numbers as the altitude distribution is quite different (see Table 1), the qualitative annual snow cycle for each region can be seen from Fig. 5. Besides the general annual behavior, the subregions exhibit some interesting features: the north-western part of the Alps shows constantly higher values of SCA due to higher elevations while the south-western part (comparable in terms of altitudinal distribution) shows lower values in winter and relatively high values starting in April. The SCA decrease in the south-west and north-west, hosting the highest elevations, however, seems to be slightly slower than in the eastern regions by virtue of the melting process being decelerated as elevation increases. Obviously, the snow persistence varies in different elevations as onset of snow melt is naturally postponed with increases in the terrain elevation. Generally, the spread is highest from November through March but it varies among the four regions: the inter-annual variability in the north-west and south-west seems to be least pronounced (e.g., 10 % in the north-west in January) resulting in a lower IQR than in the eastern regions (e.g., 20 % in the north-east in January).

4.4 Inter-annual variation of snow cover (1991–2011)

In this section, we focus on the year-to-year variability of the snow cover, as it has repeatedly been shown to be considerable (Scherrer et al., 2004). The annual pixel-wise departures from the long-term mean (1991–2011) are displayed in Fig. 6 for the entire Alpine region. The highest regions (> 2900 m a.s.l.) in the central Alps exhibit stable snow cover and the anomalies constantly lie within the uncertainty range of ±10 days. It can be further assumed that the SCD in the years 1998, 2002 and 2003 was below average, with 2007 being the poorest winter on record. In contrast, comprehensive above-average snow cover conditions are found in 1992, 1993, 2009 and 2010.

TCD
7, 3001–3042, 2013

It is striking that some anomaly patterns seem to occur systematically: firstly, a uniform pattern with above- (below-) average snow conditions, which prevail over the entire Alps (e.g., 1992, 1998, 2002 and 2007). Secondly, a pronounced north-south pattern can be observed in 1991, 1994 and 2005 when the Alpine ridge roughly divides the anomalies in a positive and a negative region. A third pattern follows an altitudinal gradient, for example in 2003, 2006, 2008 and 2009. Lower levels clearly show below- (above-) average conditions while the higher the altitudinal levels approach average conditions. Fourth, an east-west pattern, characterized by a meridional anomaly gradient, is presumed in 1996, 2000, 2004 and 2010.

Hence, the regions and altitudes were investigated in more detail as the varying climatic features seem to have a major influence on the snow cover distribution. Figure 7 illustrates the annual departures from the 1991–2011 median value (as it does not follow a normal distribution) for the three parameters SCD, SCOD and SCMD for each region with an altitudinal resolution of 100 m (from 700 to 2500 m, which corresponds to the altitude levels experiencing seasonal snow cover). Generally it can be observed, that the altitudinal variation is more pronounced in SCMD while the variability in the snow onset is lower between different altitudes. The year-to-year variability though, was found to be higher in the SCOD for all altitudes as concluded from the IQR plot (figure not shown) where the spread for SCOD was much larger than for SCMD.

A closer look at the altitudinal distribution of variation reveals that the variability at lower regions (displayed in bluish colors in Fig. 7) is increased in comparison to the values of higher altitudes (red colors). This again implies the strong dependency of snow cover variation on the vertical temperature gradient as the likelihood of frequent transitions over freezing point is highest at lower elevations.

Regarding the inter-regional differences, some interesting features become visible. Besides the lower altitudes, the inter-annual spatial variations are more apparent in the southern regions of the Alps, where the SCD and SCMD parameters especially show a higher spread in the higher regions (i.e., south-west and south-east in 2002 and 2010). Furthermore, the pronounced anomalies in the lower regions (+40 days

TCD
7, 3001–3042, 2013

SCD) in 1996 only affected the eastern part of the Alps. In the case of 1998, all regions show increased negative low-altitude anomalies and positive high-altitude anomalies, except for the south-eastern parts.

As these annual values are not affected by a cyclic (seasonal) pattern and no significant autocorrelation has been found, simple linear trends were estimated and tested for significance for each altitudinal range and each region. Most of them showed a decreasing tendency but were found to be insignificant, including the trends for the Alpine region as a whole. For some particular altitudes in single regions, however, evidence for decreasing (or increasing) values was found. These mostly affected the lowest (and partially also the highest) altitudes in the southern regions: for SCD, a slight evidence against the null hypothesis ($0.05 < p < 0.1$) was found in SW at altitudes 700–900 (trend = −2.1 days yr^{-1}) and 2100–2300 (trend = −1.2 days yr^{-1}) as well as in SE at altitudes 700 and 800 (trend = −1.7/−1.8 days yr^{-1}). Concerning SCOD, slight evidence for a later snow onset was also found in the lowest (900–1100) and highest altitude (2100–2300) levels in SW and SE. For altitudes 700–900, even moderate evidence ($p < 0.05$) was found, implying a significant trend of +0.9 days yr^{-1}. Also for the SE, significant trends ($p < 0.05$) toward a later snow onset in the lower altitudes (700–1200) were found (with trends around +1 day yr^{-1}). In summary and even though the time series is comparatively short, the lowest regions of the southern Alps seem to be the most affected by climate change over the last 20 yr while the changes in northern and more elevated parts do not show any significant tendency.

4.5 Timeseries of SCA (1985–2011)

Finally, an SCA time series analysis based on monthly data was carried out. To demonstrate the temporal stability of the SCA dataset derived from several generations of AVHRR sensors, monthly mean values from the satellite-derived SCA were compared to the same variable derived from the gridded station dataset (available December–May, 1989–2009, for Switzerland). The results are displayed in Fig. 8. A high consistency is found, not only for the relative dynamic of the SCA, but also for the absolute numbers of monthly mean values, especially in the years after 2001. The satellite record even captures small features such as the two SCA peaks in the winters 1991, 2007 or 2008. A slight overestimation of satellite-derived SCA compared to ground SCA is found in 1992 and 1993, however, and in 1995 and 1999 the satellite SCA seems not to resolve the highest peaks in January and February. In 1990, the real snow cover onset is found to be somewhat shifted to earlier dates in the satellite data but the absolute numbers of the winter maximum, lying at 50 %, are well represented.

The irregular distribution of AVHRR data (cf. Fig. 2) needs special attention before time series analysis. Therefore, we tested whether the increasing availability of scenes influences the accuracy of the monthly values. This was done by artificially reducing the number of scenes in 2002–2011 to the level of 1990–2000 when only one satellite was in orbit at a time. The obtained monthly mean values are over-plotted in red in the upper graph and the absolute differences between the two datasets are shown in the lower graph in Fig. 8. Except for three outliers, 95 % of the values lie within ±6 %. Overall, the monthly mean values do not significantly differ (t tested, $p = 0.8$). The mean difference lies at 1.1 % with a standard deviation of 3.6 %. Therefore, it is concluded that the data distribution does not have an essential influence on the derived snow climatology. In addition, we hypothesize that the slightly advanced sensor technology of AVHRR/3, operating on N16 to N19 from 2002 onwards, rather than the data disposability, is responsible for the high agreement with the ground data in Fig. 8 after 2002.

Having assessed the accuracy and consistency of the satellite record, a 27 yr time series of SCA was compiled and analyzed for the whole extent of the Alpine region. As missing values were inevitable due to satellite data unavailability, data gaps (namely three months in 1995 and four months in 2001) were filled by the long-term mean value of the respective months. The pronounced seasonal cycle of snow cover (see also Fig. 8) was removed by using the monthly standardized anomalies.

It has been shown that the precision of trend estimates in environmental data is critically influenced by the variability and autocorrelation of the underlying noise process (Tiao et al., 1990). In particular, autocorrelation tends to interact with the linear trend and therefore increases the length of the time series required to detect a certain trend (Weatherhead et al., 1998). The necessary length of record (monthly data) can therefore be assessed by investigating the standard deviation and the autocorrelation of the residuals after the seasonal component has been removed (i.e., the standardized anomalies).

As expected, the autocorrelation of the time series (residuals) is significant (> 0.5 lag-1) and the standard deviation of the residuals is $\sigma = 7.9$. Applying the Eq. (3) in Weatherhead et al. (1998), we calculated the number of years of data required to detect a real trend of a certain magnitude. Using the autocorrelation and variation of the time series residuals, this results in a minimum length of time period of 21 yr to detect a significant trend of the magnitude of 5 % per decade. A time period of approximately 61 yr would be required to detect a less strong but significant trend of 1 % per decade (always at a 90 % confidence level) for the SCA parameter. Therefore, we conclude, that (depending on the magnitude of trend) the time series should be analyzed for trends with care.

Figure 9 illustrates the monthly SCA standardized anomalies derived from the satellite record over the European Alps (1985–2011). The respective regression parameters and the autocorrelation value are provided in Table 2. As has been observed in Fig. 6, the years 1988–1990, 2002 and 2007 are extreme with a relatively small SCA. On the contrary, the years 1991, 1992, 2005, 2009 and 2010 represent years with relatively high SCA values. Concerning the Alpine region as a whole, no statistically significant trend ($p = 0.7$) in SCA over the last 27 yr was found in annual SCA in the Alpine region.

To revisit the regional issue, the same analysis was carried out for all subregions (the absolute SCA time series for each region are plotted in Fig. A1 in the Appendix). The standardized monthly anomalies are illustrated in Fig. 10. No significant trends were found here either, as can be seen from Table 2, which summarizes the regression parameters and the autocorrelation values for each region separately. Slight differences in the anomalies are still apparent between the subregions (e.g., in 1994 and 1996) and although not significant, the linear trend-lines tend towards increasing SCA in the northern parts and towards decreasing SCA in the south-western region with a decadal trend of −0.04 standard deviations (cf. Table 2).

5 General discussion

The above findings generally indicate that alpine snow cover is highly variable in time and space. Due to its medium resolution of 1 km, this record is not able to investigate small scale features such as snowline dependence on aspect as a pixel in complex terrain typically includes various aspects. Rather, it is intended to capture the relative large scale snow dynamics that seem to be well reproduced. Four patterns relating to spatial anomaly occurrence were suggested: uniform, altitudinal, meridional and zonal. On the regional scale, these patterns generally agree with the findings by Laternser and Schneebeli (2003) who presented three priorities on which the degree of snowiness in Switzerland is based: first, *time*, with periods of abundant or poor snow conditions spanning large areas. Due to the relative brevity of the record, this pattern is not as obvious here but presumably resembles the first pattern. Second, *space*, with distinct regions showing more or less pronounced anomalies such as the north-south pattern found here. And third, *altitude* with relative differences in anomalies along altitudinal steps. Analogous patterns were also found by Scherrer and Appenzeller (2006). In their investigations, they identified three major patterns of large-scale snow variability for Switzerland (for the parameters December-January-February period new snow sum, snow depth and snow days): uniform, north-south and low-high altitude. However, both studies were restricted to the area of Switzerland, that is they were located – as defined here – mostly in the north-west and minor parts in the south-west. Upon extending the analysis to the entire Alpine region, an east-west gradient also becomes apparent in this study.

The results obtained from the novel satellite-based SCA time series reveal interesting details on the temporal distribution of the snow cover extent in the Alpine region over the last 27 yr. Indeed, many long-term in situ snow climatologies in different regions have been analyzed investigating different snow parameters, generally showing a significant decrease of snow abundance (Marty, 2008; Beniston, 1997; EEA, 2009; Durand et al., 2009) particularly at lower altitudes. Most of them, however, analyze earlier periods or smaller areas than the record presented here. The 1990s were previously found to be the years with the lowest new snow sums and snow days on record (Laternser and Schneebeli, 2003) while the newest results show that the snow conditions seem to have partly recovered since 2000, especially at low elevations (Scherrer et al., 2010; Valt and Cianfarra, 2010). Recently, Scherrer et al. (2013) even showed that the strongly decreasing trends found in the late 1980s and 1990s are followed by a trend reversal in the last 10 yr (2000–2009), which was attributed to a recent "plateauing" or even slightly decreasing temperatures in Switzerland. Apparently, this behavior could be appropriately reproduced in the satellite record and seems to apply to the whole Alpine region. Furthermore, this may explain the absence of a significant trend in the standardized SCA anomalies. Therefore, our results do not conflict with previous findings but may also indicate – confirming the findings by Scherrer et al. (2013) – a deceleration of the decreasing snow trend in the Alpine region, even though the time period is comparatively short. Yet, indications towards a shorter SCD in lower regions in the southern parts were found.

Finally, on the hemispheric scale, the AVHRR snow time series is in good agreement with the satellite-based snow cover climatology of the Northern Hemisphere (NH) weekly updated at the Rutgers Snow Lab (http://climate.rutgers.edu/snowcover/, accessed March 2013). This climatology also suggests a weakening (even a reversal in the DJF) in the negative trend found for the period under investigation here. Unfortunately, the prominent abrupt shift in NH snow cover extent in the 1980s, described in (Robinson and Frei, 2000), lies beyond the length of this record. Nevertheless, the major advantage of this record, compared to similar products such as Moderate Resolution Imaging Spectroradiometer (MODIS) or (Advanced) Along-Track Scanning Radiometer ((A)ATSR), is its unique length. Likewise, the relatively high spatial resolution compared to existing long-term satellite records such as the Rutgers snow lab prod-

TCD
7, 3001–3042, 2013

uct (24 km) enables snow cover investigations even in complex terrain where 1 km is required as a minimum.

6 Conclusions

In this study, we presented a novel 1 km satellite-based snow cover dataset for the Alpine region. The first objective was to generate a new set of cloud-free satellite snow products for use in climate research. This was done using a cloud gap-filling technique based on a combination of spatial and temporal compositing. Thereby, the amount of cloud could be substantially reduced and a comparison of the composite product with gridded station data suggests good accuracy. Furthermore, critical issues such as data record length or irregular data availability, potentially affecting the consistency and significance of the dataset, were addressed. Based on the relation between the auto-correlation and the standard deviation of the residuals (see Weatherhead et al., 1998), the length of the recorded period is concluded to be sufficient for limited magnitudes of the trend for the SCA parameter. By artificially reducing the data availability to the level of one satellite in orbit at a time, it was shown that the values almost exactly coincide with the SCA derived from the full dataset. Consequently, we assume data availability as having no essential influence on the SCA climatology. Yet, small data gaps, pixel missclassifications or cloud persistence longer than the filling period (10 days here) inevitably introduce minor errors in parameters such as SCOD, SCD or SCMD.

Based on this dataset, the second objective was to investigate spatiotemporal distribution of snow cover in the European Alps over the last 27 yr (21 yr for spatial applications) from the satellite perspective. The long-term mean spatial representation of SCD, SCOD and SCMD showed a strong correlation of these parameters with altitude due to the vertical temperature gradient. However, regional differences became apparent, especially between the northern and the southern parts of the Alpine main crest, but also along the east-west direction. Similar patterns, namely uniform, altitudinal, meridional and zonal, were found in the annual departures of SCD from the long-term mean for

TCD
7, 3001–3042, 2013
A satellite-based snow climatology
F. Hüsler et al.

the period 1991–2011. Regional analyses indicated significant trends towards shorter SCD at low elevations (700–900 m a.s.l.) in the south-west and south-east.

Overall, the analysis of the 27 yr SCA monthly mean time series (1985–2011) indicated no significant linear trend for the entire Alpine region. The same is true for regional analyses even though some tendencies toward increasing (decreasing) SCD in the northern (southern) parts were found. Although this result is somewhat surprising in the context of an anticipated climate change, it is in accordance with other research findings.

As this study presents a broad overview on the spatiotemporal snow cover variability, it also implies the need for more detailed investigations. For example, future work could be directed towards seasonal trend analysis. It is also recommended to focus on large-scale atmospheric modes of climate variability (North Atlantic Oscillation or Arctic Oscillation), that were found to have a certain influence on European snow cover (Bartolini et al., 2010; Kim et al., 2012). In addition, the use of a simple degree-day approach or the 0-degree isotherm might be included in the analysis to discern the influence of temperature and precipitation on snow cover variability. Furthermore, the SCMD data may feature an interesting bridge to the analysis of future alpine plant growth as this parameter was found to be highly correlated to the timing of snow melt-out (Rammig et al., 2010).

Following the above considerations, these results establish the confidence in RS products for the purpose of long-term snow applications as we succeeded in (a) suppressing the influence of changing sensors and increasing data availability and (b) the gap filling methods seem to work well. Both, (a) and (b) raise confidence in the data set and demonstrate the valuable role of a long-term satellite-based snow climatology for complementing in situ time series. This study is therefore considered an important contribution to a regional climate observing system. Basically, the methodology used to compile this dataset could be applied to other regions of the world with sparser ground data than the Alpine region. Nevertheless, this critically depends on the availability of long-term AVHRR archives at the sensor's full spatial resolution. An extension of the data set to cover whole Europe is planned within the scope of the Globsnow-2 project funded by the European Space Agency (ESA). Finally, this novel data record bears the potential to serve as a reference for climate models, in which snow cover is still not adequately represented, and to provide spatially and temporally comprehensive information for related research fields.

Acknowledgements. The AVHRR 1 km data were partially acquired from the NOAA Comprehensive Large Array-data Stewardship System (CLASS; http://class.noaa.gov), the German Aerospace Center (DLR) and the Freie Universität Berlin. Special thanks go to Dirk Koslowsky. The authors wish to express their gratitude to Richard Armstrong and Nando Foppa for their valuable inputs on the manuscript. This work was funded by the Hyper-Swiss-Net and the ESA Globsnow-2 project.

References

Agrawala, S.: Climate Change in the European Alps: Adapting Winter Tourism and Natural Hazards Management, Organisation for Economic Co-operation and Development, 2007. 3003

Armstrong, R. L. and Brodzik, M. J.: Recent Northern Hemisphere snow extent: a comparison of data derived from visible and microwave satellite sensors, Geophys. Res. Lett., 28, 3673–3676, 2001. 3004, 3009

Auer, I., Böhm, R., Jurkovic, A., Lipa, W., Orlik, A., Potzmann, R., Schöner, W., Ungersböck, M., Matulla, C., Briffa, K., Jones, P., Efthymiadis, D., Brunetti, M., Nanni, T., Maugeri, M., Mercalli, L., Mestre, O., Moisselin, J.-M., Begert, M., Müller-Westermeier, G., Kveton, V., Bochnicek, O., Stastny, P., Lapin, M., Szalai, S., Szentimrey, T., Cegnar, T., Dolinar, M., Gajic-Capka, M., Zaninovic, K., Majstorovic, Z., and Nieplova, E.: HISTALP-historical instrumental climatological surface time series of the Greater Alpine Region, Int. J. Climatol., 27, 17–46, doi:10.1002/joc.1377, 2007. 3005, 3006, 3030, 3032

Auer, M., Meister, R., Stoffel, A., and Weingartner, R.: Analyse und Darstellung der mittleren monatlichen Schneehöhen in der Schweiz, Wasser–Energie–Luft, 7/8, 173–178, 2004. 3007

TCD
7, 3001–3042, 2013
A satellite-based snow climatology
F. Hüsler et al.

Bartolini, E., Claps, P., and D'Odorico, P.: Connecting European snow cover variability with large scale atmospheric patterns, Adv. Geosci., 26, 93–97, doi:10.5194/adgeo-26-93-2010, 2010. 3022

Beniston, M.: Variations of snow depth and duration in the Swiss Alps over the last 50 years: links to changes in large-scale climatic forcings, Climatic Change, 36, 281–300, 1997. 3003, 3020

Cihlar, J., Latifovic, R., Chena, J., Trishchenko, A., Duc, Y., Fedosejevsa, G., and Guindona, B.: Systematic corrections of AVHRR image composites for temporal studies, Remote Sens. Environ., 89, 217–233, doi:10.1016/j.rse.2002.06.007, 2004. 3004

Dietz, A. J., Kuenzer, C., Gessner, U., and Dech, S.: Remote sensing of snow – a review of available methods, Int. J. Remote Sens., 33, 4094–4134, doi:10.1080/01431161.2011.640964, 2012. 3004

Durand, Y., Giraud, G., Laternser, M., Etchevers, P., Mérindol, L., and Lesaffre, B.: Reanalysis of 47 years of climate in the French Alps (1958–2005): climatology and trends for snow cover, J. Appl. Meteorol. Climatol., 48, 2487–2512, doi:10.1175/2009JAMC1810.1, 2009. 3020

EEA: Regional climate change and adaptation, Tech. rep., European Environmental Agency, doi:10.2800/12552, 2009. 3003, 3020

Elsasser, H. and Bürki, R.: Climate change as a threat to tourism in the Alps, Clim. Res., 20, 253–257, doi:10.3354/cr020253, 2002. 3003

Fontana, F. M. A., Trishchenko, A. P., Luo, Y., Khlopenkov, K. V., Nussbaumer, S. U., and Wunderle, S.: Perennial snow and ice variations (2000–2008) in the Arctic circumpolar land area from satellite observations, J. Geophys. Res., 115, F04020, doi:10.1029/2010JF001664, 2010. 3013

Foppa, N. and Seiz, G.: Inter-annual variations of snow days over Switzerland from 2000–2010 derived from MODIS satellite data, The Cryosphere, 6, 331–342, doi:10.5194/tc-6-331-2012, 2012. 3004, 3007, 3008, 3009

Fuchs, S. and Brandl, M.: Damage potential and losses resulting from snow avalanches in settlements of the Canton of Grisons, Switzerland, Nat. Hazards, 34, 53–69, doi:10.1007/s11069-004-0784-y, 2005. 3003

Gafurov, A. and Bárdossy, A.: Cloud removal methodology from MODIS snow cover product, Hydrol. Earth Syst. Sci., 13, 1361–1373, doi:10.5194/hess-13-1361-2009, 2009. 3008

Gao, J., Williams, M. W., Fu, X., and Gong, T.: Spatiotemporal distribution of snow in eastern Tibet and the response to climate change, Remote Sens. Environ, 121, 1–9, doi:10.1016/j.rse.2012.01.006, 2012. 3009

Gutman, G. and Masek, J. G.: Long-term time series of the Earth's land-surface observations from space, Int. J. Remote Sens., 33, 4700–4719, doi:10.1080/01431161.2011.638341, 2012. 3004

Hall, D. K., Riggs, G. A., Foster, J. L., and Kumar, S. V.: Development and evaluation of a cloud-gap-filled MODIS daily snow-cover product, Remote Sens. Environ., 114, 496–503, doi:10.1016/j.rse.2009.10.007, 2010. 3008, 3011

Hänggi, P. and Weingartner, R.: Variations in discharge volumes for hydropower generation in Switzerland, Water Resour. Manag., 26, 1231–1252, doi:10.1007/s11269-011-9956-1, 2012. 3003

Hantel, M. and Hirtl-Wielke, L. M.: Sensitivity of Alpine snow cover to European temperature, Int. J. Climatol., 27, 1265–1275, doi:10.1002/joc.1472, 2007. 3003

Heidinger, A. K., Straka, W. C., Molling, C. C., Sullivan, J. T., and Wu, X. Q.: Deriving an inter-sensor consistent calibration for the AVHRR solar reflectance data record, Int. J. Remote Sens., 31, 6493–6517, doi:10.1080/01431161.2010.496472, 2010. 3004

Hüsler, F., Fontana, F., Riffler, M., Neuhaus, C., Musial, J., and Wunderle, S.: AVHRR archive and processing facility at the University of Bern: a comprehensive 1 km satellite data set for climate change studies, EARSeL eproc., 10, 83–101, 2011. 3006

Hüsler, F., Jonas, T., Wunderle, S., and Albrecht, S.: Validation of a modified snow cover retrieval algorithm from historical 1 km AVHRR data over the European Alps, Remote Sens. Environ., 121, 497–515, doi:10.1016/j.rse.2012.02.018, 2012. 3004, 3006, 3007

IPCC: Climate Change 2007: The Physical Science Basis, Tech. rep., Intergovernmental Panel on Climate Change (IPCC), Geneva, Switzerland, 2007. 3003

James, M. E. and Kalluri, S. N.: The Pathfinder AVHRR land data set: an improved coarse resolution data set for terrestrial monitoring, Int. J. Remote Sens., 15, 3347–3363, 1994. 3004

Jasper, K., Gurtz, J., and Lang, H.: Advanced flood forecasting in Alpine watersheds by coupling meteorological observations and forecasts with a distributed hydrological model, J. Hydrol., 267, 40–52, doi:10.1016/S0022-1694(02)00138-5, 2002. 3003

Jonas, T., Rixen, C., Sturm, M., and Stöckli, V.: How alpine plant growth is linked to snow cover and climate variability, J. Geophys. Res.-Biogeo., 113, G03013, doi:10.1029/2007JG000680, 2008. 3003, 3013

Jonas, T., Marty, C., and Magnusson, J.: Estimating the snow water equivalent from snow depth measurements in the Swiss Alps, J. Hydrol., 378, 161–167, doi:10.1016/j.jhydrol.2009.09.021, 2009. 3007

Jones, J.: Habitat selection studies in avian ecology: a critical review, Auk, 118, 557–562, 2001. 3003

Khlopenkov, K. V. and Trishchenko, A. P.: SPARC: new cloud, snow, and cloud shadow detection scheme for historical 1 km AVHRR data over Canada, J. Atmos. Ocean. Tech., 24, 322–343, 2007. 3006

Kim, Y., Kim, K.-Y., and Kim, B.-M.: Physical mechanisms of European winter snow cover variability and its relationship to the NAO, Clim. Dynam., 40, 1657–1669, doi:10.1007/s00382-012-1365-5, 2012. 3022

König, M., Winther, J.-G., and Isaksson, E.: Measuring snow and glacier ice properties from satellite, Rev. Geophys., 39, 1–27, doi:10.1029/1999RG000076, 2001. 3004

Laternser, M. and Schneebeli, M.: Long-term snow climate trends of the Swiss Alps (1931–99), Int. J. Climatol., 23, 733–750, 2003. 3003, 3019, 3020

Lehning, M., Völksch, I., Gustafsson, D., Nguyen, T. A., Stähli, M., and Zappa, M.: ALPINE3D: a detailed model of mountain surface processes and its application to snow hydrology, Hydrol. Process., 2128, 2111–2128, doi:10.1002/hyp.6204, 2006. 3003

Magnusson, J., Farinotti, D., Jonas, T., and Bavay, M.: Quantitative evaluation of different hydrological modelling approaches in a partly glacierized Swiss watershed, Hydrol. Process., 25, 2071–2084, doi:10.1002/hyp.7958, 2011. 3003

Marks, D., Domingo, J., Susong, D., Link, T., and Garen, D.: A spatially distributed energy balance snowmelt model for application in mountain basins, Hydrol. Process., 13, 1935–1959, doi:10.1002/(SICI)1099-1085(199909)13:12/13<1935::AID-HYP868>3.0.CO;2-C, 1999. 3003

Marty, C.: Regime shift of snow days in Switzerland, Geophys. Res. Lett., 35, L12501, doi:10.1029/2008GL033998, 2008. 3003, 3020

Marty, C. and Meister, R.: Long-term snow and weather observations at Weissfluhjoch and its relation to other high-altitude observatories in the Alps, Theor. Appl. Climatol., 110, 573–583, doi:10.1007/s00704-012-0584-3, 2012. 3003

Metsämäki, S., Mattila, O.-P., Pulliainen, J., Niemi, K., Luojus, K., and Böttcher, K.: An optical reflectance model-based method for fractional snow cover mapping applicable to continental scale, Remote Sens. Environ., 123, 508–521, doi:10.1016/j.rse.2012.04.010, 2012. 3004

Nolin, A. W.: Recent advances in remote sensing of seasonal snow, J. Glaciol., 56, 1141–1150, doi:10.3189/002214311796406077, 2011. 3004

Parajka, J. and Blöschl, G.: Validation of MODIS snow cover images over Austria, Hydrol. Earth Syst. Sci., 10, 679–689, doi:10.5194/hess-10-679-2006, 2006. 3007

Parajka, J. and Blöschl, G.: Spatio-temporal combination of MODIS images-potential for snow cover mapping, Water Resour. Res., 44, W03406, doi:10.1029/2007WR006204, 2008. 3008

Parajka, J., Pepe, M., Rampini, A., Rossi, S., and Blöschl, G.: A regional snow-line method for estimating snow cover from MODIS during cloud cover, J. Hydrol., 381, 203–212, doi:10.1016/j.jhydrol.2009.11.042, 2010. 3008

Rammig, A., Jonas, T., Zimmermann, N. E., and Rixen, C.: Changes in alpine plant growth under future climate conditions, Biogeosciences, 7, 2013–2024, doi:10.5194/bg-7-2013-2010, 2010. 3022

Rango, A. and Martinec, J.: Revisiting the degree-day method for snowmelt computations, Water Resour. Bull., 31, 657–669, 1995. 3003

Rees, W. G.: Remote Sensing of Snow and Ice, CRC Press, 2005. 3004

Rhyner, J., Bründl, M., Etter, H. J., Steiniger, M., Stöckli, U., Stucki, T., Zimmerli, M., and Amman, W.: Avalanche warning Switzerland – consequences of the avalanche winter 1999, in: Proceedings of the 13th Int. Snow Science Workshop, Penticton, BC, Canada, 2002. 3007

Robinson, D. A. and Frei, A.: Seasonal variability of Northern Hemisphere snow extent using visible satellite data, Prof. Geogr., 582, 307–314, 2000. 3004, 3020

Romanov, P., Gutman, G., and Csiszar, I.: Satellite-derived snow cover maps for North America: accuracy assesement, Adv. Space Res., 30, 2455–2460, 2002. 3007

Scherrer, S. C. and Appenzeller, C.: Swiss Alpine snow pack variability: major patterns and links to local climate and large-scale flow, Clim. Res., 32, 187–199, doi:10.3354/cr032187, 2006. 3003, 3019

Scherrer, S. C., Appenzeller, C., and Laternser, M.: Trends in Swiss Alpine snow days: the role of local- and large-scale climate variability, Geophys. Res. Lett., 31, L13215, doi:10.1029/2004GL020255, 2004. 3003, 3014

TCD
7, 3001–3042, 2013

A satellite-based snow climatology

F. Hüsler et al.

Scherrer, S. C., Wüthrich, C., Croci-Maspoli, M., Weingartner, R., and Appenzeller, C.: Analyses of newly digitized and reconstructed snow series over the last 100+ years in Switzerland, in: European Conference on Applied Climatology, Zürich, 2010. 3020

Scherrer, S. C., Wüthrich, C., Croci-Maspoli, M., Weingartner, R., and Appenzeller, C.: Snow variability in the Swiss Alps 1864–2009, Int. J. Climatol., pp. n/a–n/a, doi:10.1002/joc.3653, 2013. 3020

Tiao, G. C., Reinsel, G. C., Xu, D., Pedrick, J. H., Zhu, X., Miller, A. J., DeLuisi, J. J., Mateer, C. L., and Wuebbles, D. J.: Effects of autocorrelation and temporal sampling schemes on estimates of trend and spatial correlation, J. Geophys. Res., 95, 20507–20517, 1990. 3017

Valt, M. and Cianfarra, P.: Recent snow cover variability in the Italian Alps, Cold Reg. Sci. Technol., 64, 146–157, doi:10.1016/j.coldregions.2010.08.008, 2010. 3020

Voigt, S.: Advanced methods for operational mapping of Alpine snow cover using medium resolution optical satellite data, Inaugural dissertation, University of Bern, Switzerland, 2000. 3008

Wang, X. and Xie, H.: New methods for studying the spatiotemporal variation of snow cover based on combination products of MODIS Terra and Aqua, J. Hydrol., 371, 192–200, doi:10.1016/j.jhydrol.2009.03.028, 2009. 3009, 3010

Wang, X., Xie, H., and Liang, T.: Evaluation of MODIS snow cover and cloud mask and its application in Northern Xinjiang, China, Remote Sens. Environ., 112, 1497–1513, 2008. 3008

Wang, X., Xie, H., Liang, T., and Huang, X.: Comparison and validation of MODIS standard and new combination of Terra and Aqua snow cover products in Northern Xinjiang, China, Hydrol. Process., 429, 419–429, doi:10.1002/hyp.7151, 2009. 3007

Weatherhead, E. C., Reinsel, G. C., Tiao, G. C., Meng, X.-L., Choi, D., Cheang, W.-K., Keller, T., DeLuisi, J., Wuebbles, D. J., Kerr, J. B., Miller, A. J., Oltmans, S. J., and Frederick, J. E.: Factors affecting the detection of trends: statistical considerations and applications to environmental data, J. Geophys. Res., 103, 17149–17161, doi:10.1029/98JD00995, 1998. 3018, 3021

Wiscombe, W. J. and Warren, S. G.: Model for the spectral albedo of snow. I: pure snow, Engineering, 37, 2712–2733, 1980. 3006

WMO: Implementation Plan for the Global Observing System for Climate in Support of the UNFCCC (2010 Update), Tech. Rep. 1523, Global Climate Observing System, available at: http://eprints.soton.ac.uk/162953/, 2010. 3003

TCD
7, 3001–3042, 2013

A satellite-based snow climatology

F. Hüsler et al.

WMO: Systematic Observation Requirement for Satellite-based Data Products for Climate (Update 2011), GCOS-154, Tech. rep., World Meteorological Organization, 2011. 3003
Zhao, H. and Fernandes, R.: Daily snow cover estimation from Advanced Very High Resolution Radiometer Polar Pathfinder data over Northern Hemisphere land surfaces during 1982–2004, J. Geophys. Res., 114, D05113, doi:10.1029/2008JD011272, 2009. 3004

TCD
7, 3001–3042, 2013

A satellite-based snow climatology

F. Hüsler et al.

Table 1. Distinct properties of the Alps and its subregions in terms of altitude distribution, extent and climatic influence. Color encoding corresponds to Fig. 1.

region	altitude distribution	extent [km^2]	climatic features (Auer et al., 2007)
Alpine region	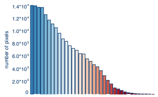	226 000	
north-west (NW)	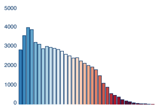	67 000	temperate westerly, oceanic features
north-east (NE)	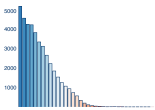	50 000	temperate westerly, continental features
south-east (SE)	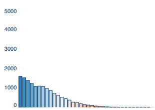	17 000	mediterranean subtropical, contintental features
south-west (SW)	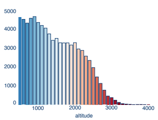	92 000	mediterranean subtropical, oceanic features

TCD
7, 3001–3042, 2013

Table 2. Regression parameters trend ϖ per decade, p value, autocorrelation φ at lag-1 and standard deviation of the residuals σ for the SCA standardized anomaly time series illustrated in Figs. 9 and 10.

region	ϖ/decade [SD]	p value	φ	σ
alps	0.02	0.77	0.55	7.9
ne	0.08	0.21	0.36	11.13
nw	0.08	0.23	0.45	8.26
se	0.03	0.62	0.49	11.17
sw	−0.04	0.55	0.50	7.77

TCD
7, 3001–3042, 2013

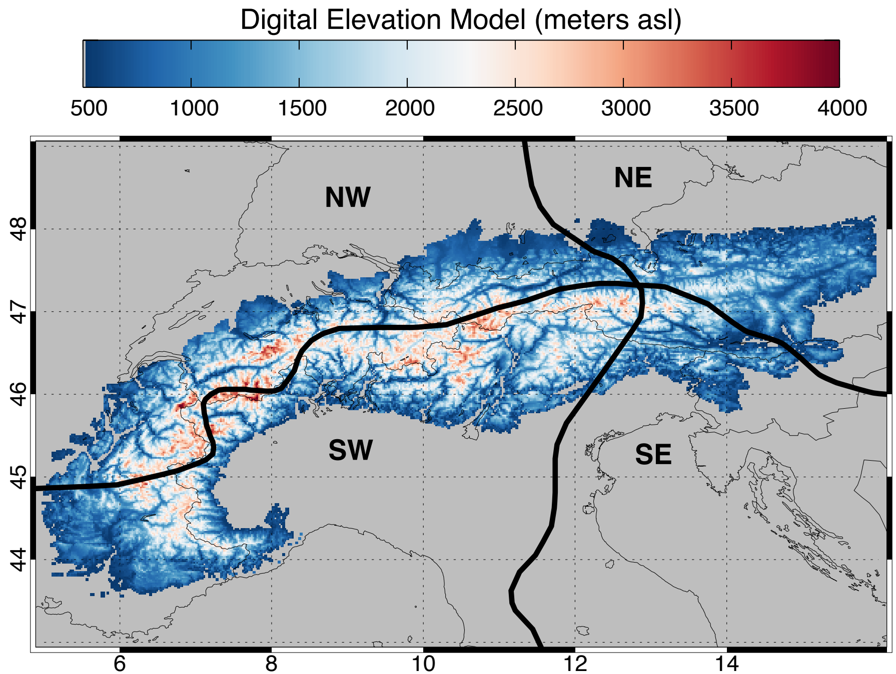

Fig. 1. Digital elevation model of the Alpine region. Bold lines indicate the subdivision into the four subregions (north-west, north-east, south-east and south-west) according to Auer et al. (2007). Data for the extra-alpine areas is not displayed.

TCD
7, 3001–3042, 2013

A satellite-based snow climatology

F. Hüsler et al.

Title Page
Abstract Introduction
Conclusions References
Tables Figures
◀▮ ▶▮
◀ ▶
Back Close
Full Screen / Esc
Printer-friendly Version
Interactive Discussion

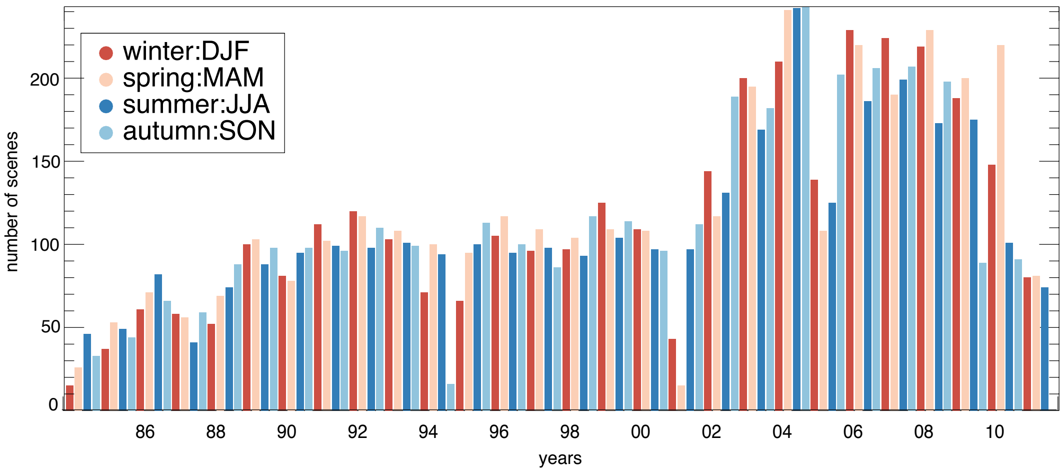

Fig. 2. Archived AVHRR overpasses illustrated by season and number of scenes for the period 1984–2011.

TCD
7, 3001–3042, 2013

A satellite-based snow climatology

F. Hüsler et al.

Title Page
Abstract Introduction
Conclusions References
Tables Figures
◀I ▶I
◀ ▶
Back Close
Full Screen / Esc
Printer-friendly Version
Interactive Discussion

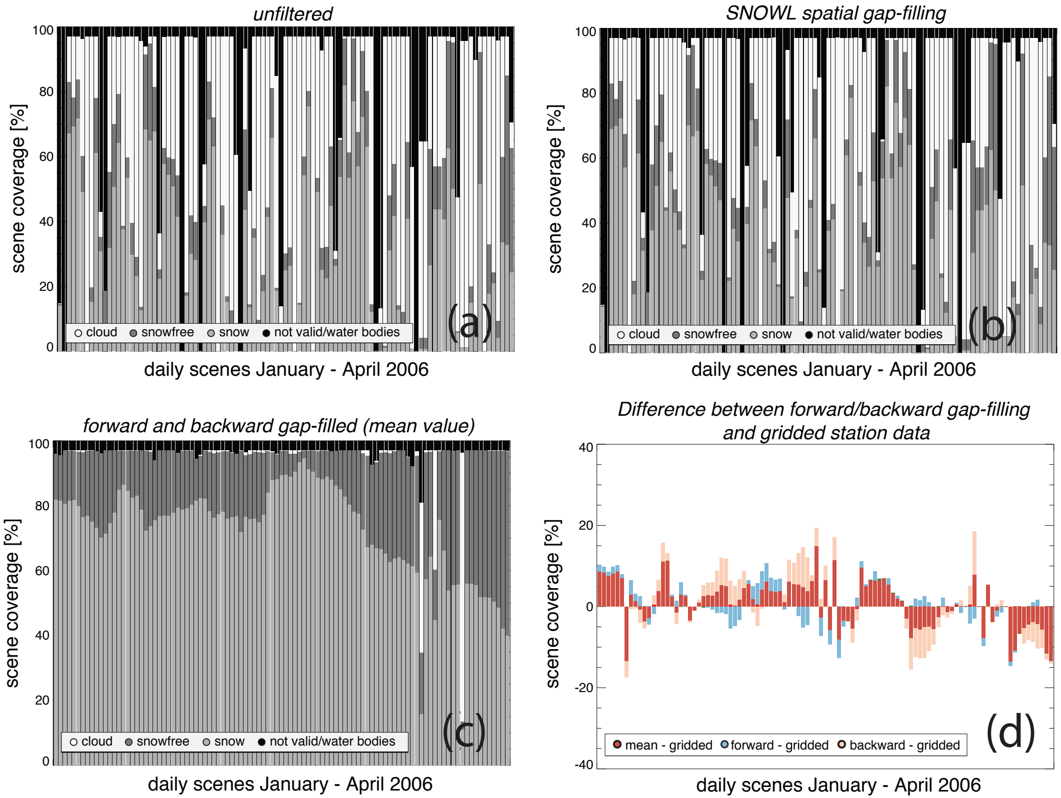

Fig. 3. Stepwise results from the spatial and temporal cloud removal process for the period January–April 2006: respective area percentage of Switzerland for the classes snow, snow-free, cloud and not valid for **(a)** unfiltered scenes, **(b)** after SNOWL spatial gap-filling filter, **(c)** after temporal backward and forward gap-filling (mean value), **(d)** differences between forward and backward direction and averaged value thereof and gridded station data.

TCD
7, 3001–3042, 2013

A satellite-based snow climatology

F. Hüsler et al.

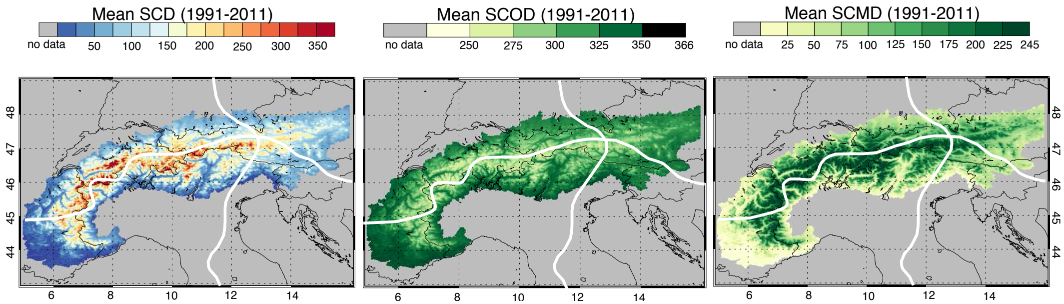

Fig. 4. Spatial representation of the long-term annual mean of snow cover parameters for the Alpine region (1991–2011): SCD (left) in numbers of snow days, SCOD (center) and SCMD (right), given as DOY for each pixel. Overall, a very strong correlation to the topography is observed but regional differences also become apparent. White lines indicate the climatic regions described in Sect. 2.1.

TCD
7, 3001–3042, 2013

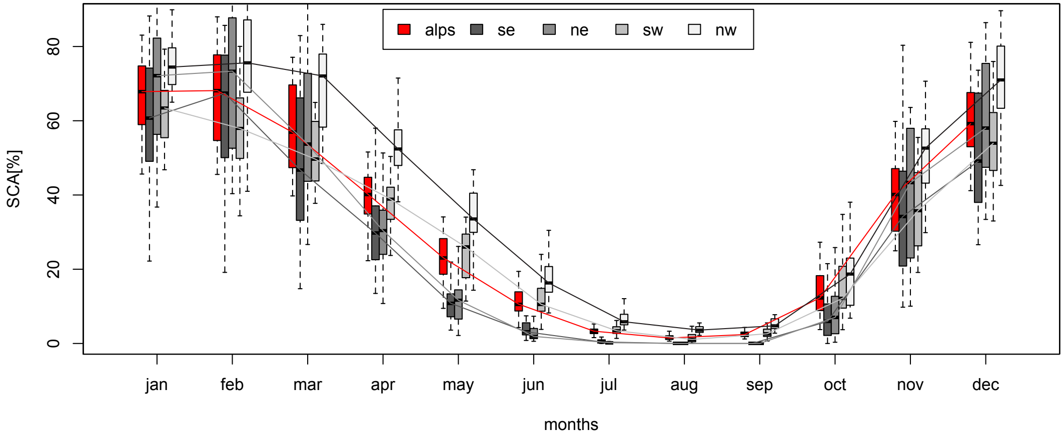

Fig. 5. Monthly median and Inter Quartile Range (IQR) of SCA averaged over the period 1985–2011 for the whole Alpine region (red) and all four subregions (gray tones) over the course of the year. SCA values are given in numbers relative to the size of the respective region (cf. Table 1). To facilitate interpretation, lines connect median values from each month.

TCD
7, 3001–3042, 2013

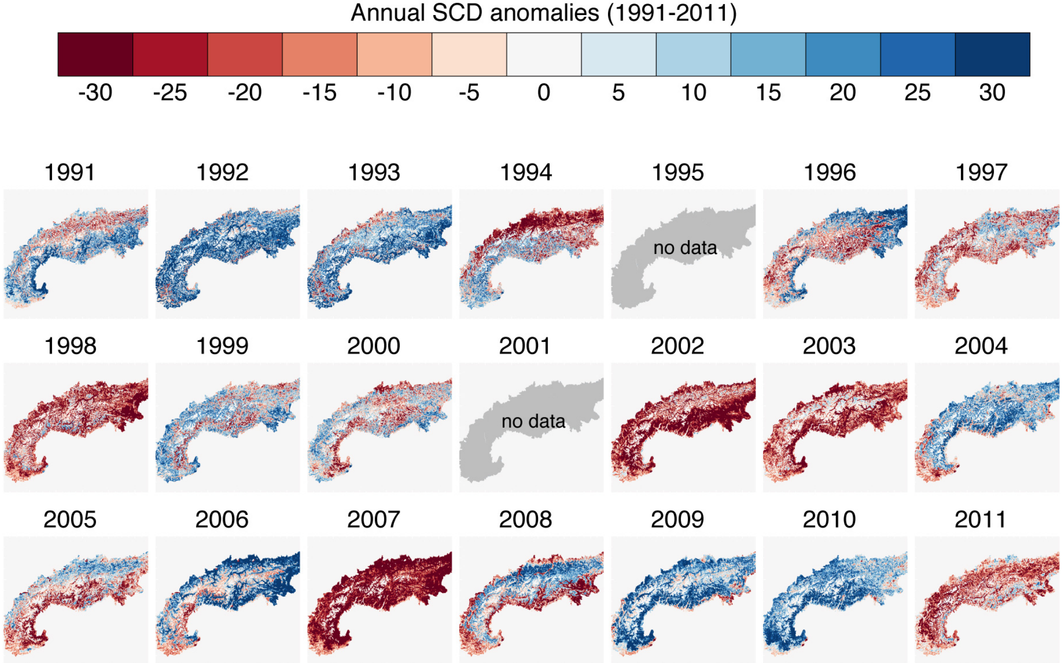

Fig. 6. Annual departures from the long-term median (1991–2011) given in days. Years refer to 1 January. The data coverage in 1995 and 2001 was insufficient for the application.

TCD
7, 3001–3042, 2013

Title Page
Abstract | Introduction
Conclusions | References
Tables | Figures
◂I | I▸
◂ | ▸
Back | Close
Full Screen / Esc
Printer-friendly Version
Interactive Discussion

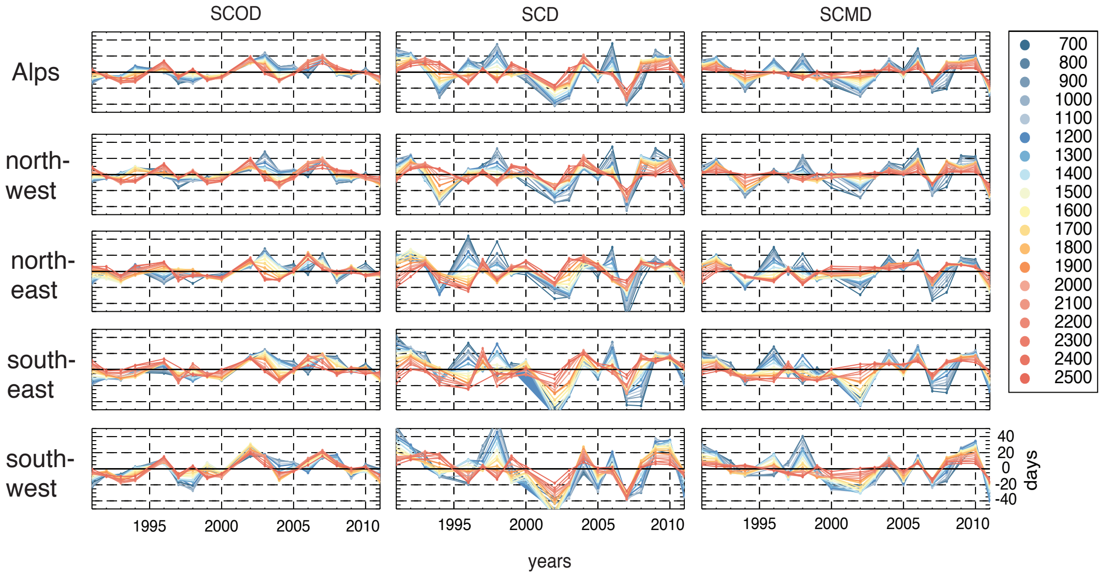

Fig. 7. Annual departures (1991–2011) of SCOD, SCD and SCMD from the long-term median for the Alpine region and all subregions given in days for different altitude levels. Years refer to 1 January. Connecting lines are displayed for easier readability of the figure only. The data coverage in 1995 and 2001 was insufficient for the application.

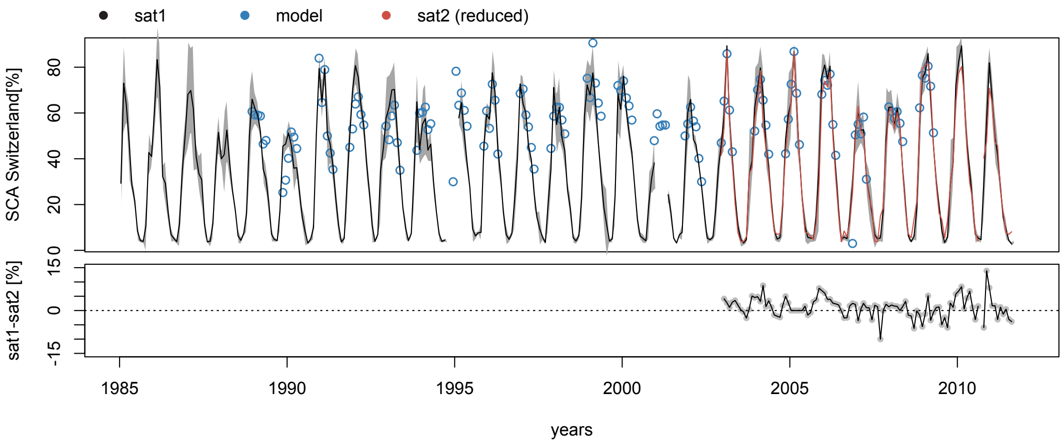

Fig. 8. Time series (1985–2011) of monthly values of SCA for Switzerland (sat1; black) including monthly standard deviation (gray shaded area) compared to the same measures derived from gridded station data (blue dots). To assess the influence of the number of data available, the dataset was artificially reduced to one satellite at the time (sat2; red). Differences between the full dataset (sat1) and the artificially reduced dataset (sat2) are illustrated in the lower graph.

TCD
7, 3001–3042, 2013

Discussion Paper | Discussion Paper | Discussion Paper | Discussion Paper |

TCD
7, 3001–3042, 2013

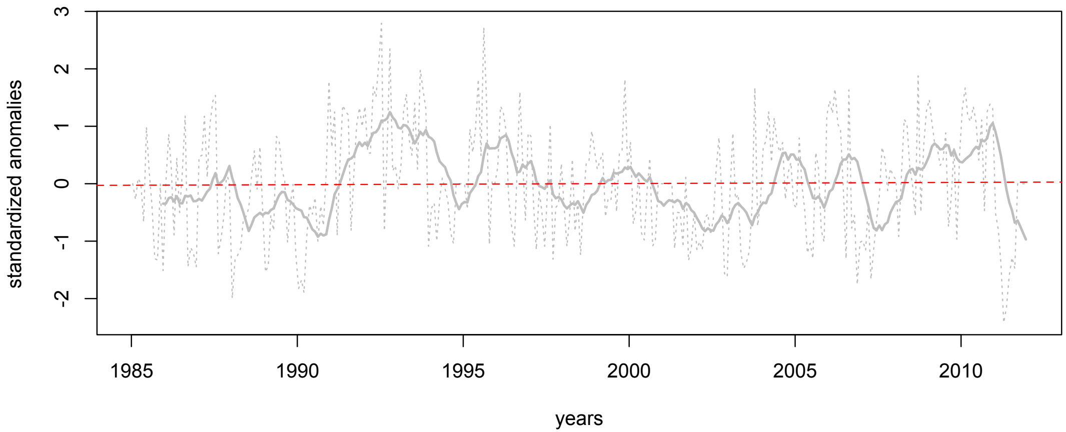

Fig. 9. Time series of Alpine region SCA monthly standardized anomalies derived from AVHRR data 1985–2011. The dotted line indicates the monthly values while the grey solid line depicts the 12 month standard moving average. The red line represents the respective linear trend.

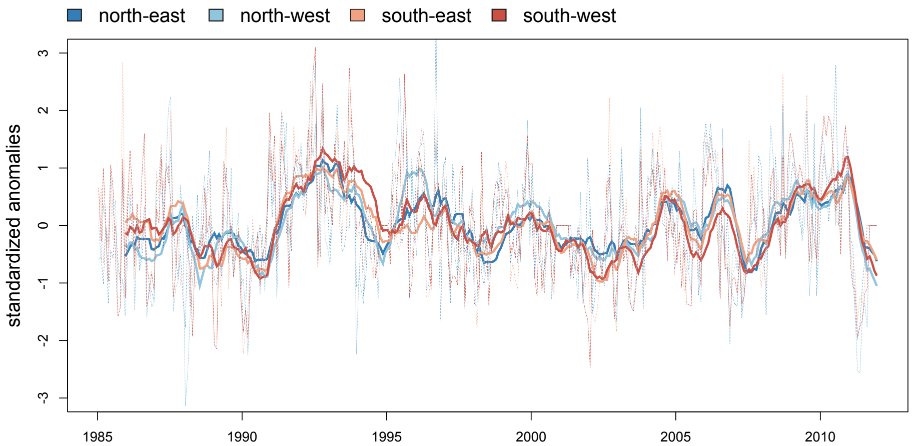

Fig. 10. Same as Fig. 9 but resolved into the four climatic regions.

Discussion Paper | Discussion Paper | Discussion Paper | Discussion Paper |

TCD
7, 3001–3042, 2013

A satellite-based snow climatology

F. Hüsler et al.

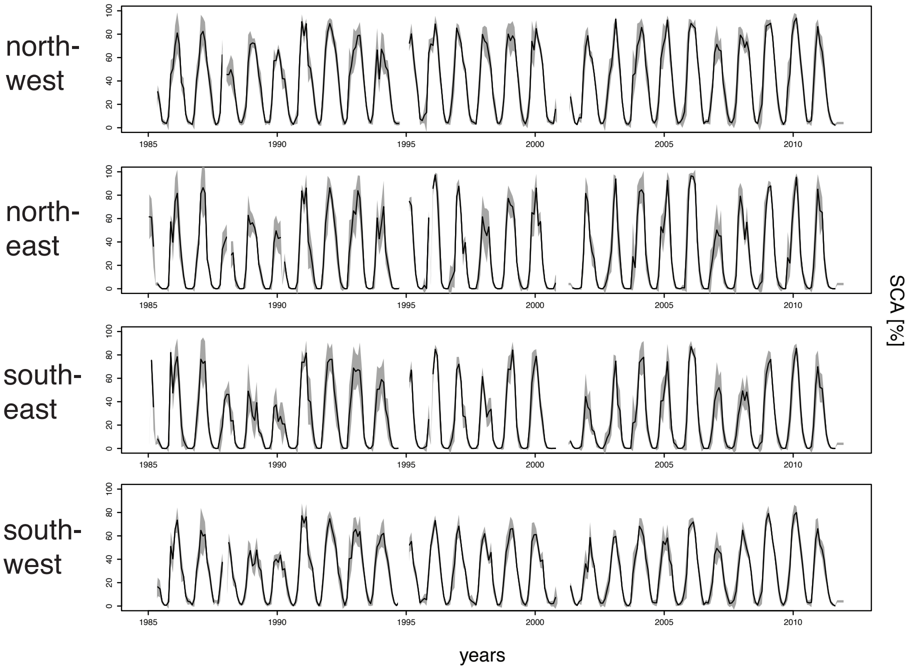

Fig. A1. Time series (1985–2011) of absolute monthly values of SCA for each region including monthly standard deviation (gray shaded area).

TCD
7, 3001–3042, 2013

A satellite-based snow climatology

F. Hüsler et al.